Electronic Supplementary Material (ESI) for New Journal of Chemistry.

A Polymeric Bis(di-*p*-anisylamino)fluorene Hole-Transport Material for Stable n-i-p Perovskite Solar Cells

Marie-Hélène Tremblay[a], Kelly Schutt[b], Yadong Zhang[a], Stephen Barlow[a], Henry J. Snaith[b], and Seth R. Marder[a*]

[a] School of Chemistry and Biochemistry, and Center for Organic Photonics and Electronics (COPE), Georgia Institute of Technology GA, Atlanta 30332-0400, United States
[b] Clarendon Laboratory, Department of Physics, University of Oxford, Parks Road, Oxford OX1 3PU, United Kingdom

***Corresponding author: Seth R. Marder, seth.marder@chemistry.gatech.edu**

Supporting Information

Table of Contents

1- Experimental Procedures

Synthesis

Molybdenum tris(1-(trifluoroacetyl)-2-(trifluoromethyl)ethane-1,2-dithiolene) (Mo(tfd-$COCF_3)_3$),[1] 5-norbornene-2-carbonyl chloride,[2] and *tert*-butyl(3-(2,7-diiodo-9-methyl-9*H*-fluoren-9-yl)propoxy)dimethylsilane[3] were synthesized according to previous reports. Other chemicals were purchased and used without further purification.

9-(3-((*tert*-Butyldimethylsilyl)oxy)propyl)-N2,N2,N7,N7-tetrakis(4-methoxyphenyl)-9-methyl-9H-fluorene-2,7-diamine (1): ^{t}BuOK (1.23 g, 11.21 mmol), *tert*-butyl(3-(2,7-diiodo-9-methyl-9*H*-fluoren-9-yl)propoxy)dimethylsilane (1 g, 1.78 mmol), and bis(4-methoxyphenyl)amine (2.04 g, 8.9 mmol) were added in a 2 necked round-bottomed flask. 18 mL of toluene was added, and the solution was deoxygenated. ^{t}Bu$_3$P (0.04 g, 0.178 mmol) and $Pd(OAc)_2$ (0.02 mg, 0.089 mmol) were then added in the solution and heated at 140 °C for 48 h under N_2. The mixture was filtered over celite and washed in CH_2Cl_2. The filtrate was partitioned between water and CH_2Cl_2 and the organic layer was washed with saturated NaCl solution, dried over Na_2SO_4, and evaporated under reduced pressure. The residue was purified by column chromatography (10% ethyl acetate in hexane) to obtain a beige oil (714 mg, 54%). ^{1}H NMR ($CDCl_3$, 400 MHz): 7.47 (d, *J* = 8.2 Hz, 2H), 7.01 (m, 10H), 6.88 (m, 8H), 6.81 (m, 2H), 3.78 (s, 12H), 3.36 (t, *J* = 6.7 Hz, 2H), 1.82 (m, 2H), 1.30 (s, 3H), 0.90 (s, 3H), 0.83 (s, 9H), 0.04 (s, 6H). ^{13}C{^{1}H} NMR ($CDCl_3$, 100 MHz): δ 155.83, 152.77, 147.61, 141.40, 133.56, 125.92, 120.54, 119.51, 115.92, 114.61, 63.05, 54.81, 50.01, 36.54, 28.15, 26.29, 25.46, 17.90, -5.93. HRMS-ESI (m/z): calcd for $C_{51}H_{58}N_2O_5Si$ (M^+), 806.4109; found, 806.4094. Anal. Calcd for $C_{51}H_{58}N_2O_5Si$: C, 75.89; H, 7.42; N, 3.47. Found: C, 75.60; H, 7.25; N, 3.42.

3-(2,7-Bis(di(4-methoxyphenyl)amino)-9-methyl-9*H*-fluoren-9-yl)propan-1-ol (2): **1** (1 g, 1.23 mmol) was dissolved in THF (0.5 mL) and a solution of tetra-*n*-butylammonium fluoride (1.0 M in THF, 2 mL) was added. The mixture was stirred at room temperature while the reaction was followed by TLC. Upon the disappearance of the protected alcohol, the solution was filtered through a silica gel plug with celite on top, which was then washed with a 1:1 hexane/ ethyl acetate mixture. The filtrate was poured into a separatory funnel containing 15 mL of water. The product was extracted with dichloromethane (3 x 5 mL). The organic layers were combined and the solvent was removed under reduced pressure. A flash chromatography column was also performed (silica gel, 3-100% ethyl acetate in hexane gradient). The solvent was removed using a rotary evaporator to yield 0.668 g (100%) of a beige powder. ^{1}H NMR (acetone-d_6, 500 MHz): δ 7.48 (d, *J* = 8.2 Hz, 2H), 7.03 (dt, *J* = 3.2, 9.0 Hz, 10H), 6.88 (dt, *J* = 3.6, 9.0 Hz, 8H), 6.81 (dd, *J* = 2.2, 8.3 Hz, 2H), 3.78 (s, 12H), 3.27 (t, *J* = 6.2 Hz, 2H), 2.80 (s, 1H), 1.84-1.18 (m, 2H), 1.29 (s, 3H), 0.93-0.88 (m, 2H). ^{13}C{^{1}H} NMR

(acetone-d_6, 126 MHz): δ 155.7, 152.7, 147.4, 141.3, 133.5, 125.8, 120.3, 119.4, 115.8, 114.5, 61.8, 54.7, 49.9, 36.6, 28.1, 26.1. HRMS-ESI (m/z): calcd for $C_{45}H_{44}N_2O_5$ (M^+), 692.3245; found, 692.3231. Anal. Calcd for $C_{45}H_{44}N_2O_5$: C, 78.01; H, 6.40; N, 4.04. Found: C, 75.75; H, 6.42; N, 3.75.

3-(2,7-Bis(dis(4-methoxyphenyl)amino)-9-methyl-9H-fluoren-9-yl)propyl bicyclo[2.2.1]hept-5-ene-2-carboxylate (**M1**): To a solution of **2** (275 mg, 0.395 mmol) and pyridine (0.1 mL) in 1 mL of dry dichloromethane, a solution 5-norbornene-2-carbonyl chloride (*exo*/*endo* mixture, 150 mg, 0.961 mmol) in 1 mL of dry dichloromethane was added dropwise under an atmosphere of argon. The reaction mixture was stirred overnight at room temperature. After completion by TLC, 10 mL of water was added to the solution and the solution was extracted 3x using dichloromethane. The crude product was purified via flash chromatography using hexanes/EtOAc (9:1 v/v) to yield a beige powder as a mixture of the endo and exo stereoisomers (263 mg, 82%). ^{1}H NMR (acetone-d_6, 700 MHz): δ 7.52 (d, *J* = 8.2 Hz, 2H), 7.05 (m, 10H), 6.90 (m, 8H), 6.83 (dd, *J* = 1.4, 8.2Hz, 2H), 6.10-5.80 (m, 2H), 3.80 (s, 12H), 3.08 (s, 1H), 2.92 (m, 1H), 3.08 (m, 3H), 1.85 (m, 3H), 1.32 (m, 7H), 1.02 (m, 2H). ^{13}C{^{1}H} NMR (acetone-d_6, 175 MHz): δ 174.4, 156.7, 153.3, 153.3, 148.6, 148.6, 142.3, 142.2, 138.2, 134.4, 133.3, 126.8, 126.7, 121.6, 121.5, 120.5, 116.9, 116.7, 115.5, 64.7, 55.7, 50.8, 50.1, 46.4, 43.8, 43.2, 42.3, 37.4, 27.1, 25.0. HRMS-ESI (m/z): calcd for $C_{53}H_{52}N_2O_6$ (M^+), 812.3820; found, 812.3797. Anal. Calcd for $C_{53}H_{52}N_2O_6$: C, 78.30; H, 6.45; N, 3.45. Found: C, 77.81; H, 6.46; N, 3.27.

P1: **M1** (358 mg, 0.44 mmol) was dissolved in anhydrous and deoxygenated dichloromethane (3 mL). Grubbs 2nd generation initiator ((Ru(PCy_3)(=CHPh)LCl_2 (Cy = cyclohexyl; L = 1,3-bis(2,4,6-trimethylphenyl)-2-imidazolidinylidene)) (3.4 mg, 0.004 mmol) was dissolved in anhydrous and deoxygenated dichloromethane (2 mL) and added quickly to the stirring monomer solution. The solution was stirred at room temperature under nitrogen for 3 h before ethyl vinyl ether (5 mL) was added; the mixture was then stirred for 1 h. The polymer was precipitated in MeOH (20 mL) and reprecipitated twice from dichloromethane and MeOH to yield a yellow powder (234 mg, 65%). ^{1}H NMR ($CDCl_3$, 500 MHz): δ 6.82 (s, 22H), 5.19 (m, 2H), 3.74 (s, 12H), 2.98 (s, 1H), 2.70 (s, 2H), 2.39 (s, 1H), 1.88 (s, 1H), 1.70 (s, 4H), 1.23 (2, 4H), 0.96 (s, 2H). M_w = 101 kDa, Đ = 1.7 (determined via GPC in $CHCl_3$). Anal. Calcd for $(C_{53}H_{52}N_2O_6)_n$: C, 78.30; H, 6.45; N, 3.45. Found: C, 77.92; H, 6.57; N, 3.46.

Characterization Techniques

Nuclear magnetic resonance (NMR). NMR measurements were conducted with a Bruker Advance IIIHD 500 and a Bruker Advance IIIHD 700 spectrometer operating at 500 MHz and 700 MHz.

Elemental analysis (EA). Elemental analyses for C, H, and N were performed by Atlantic Microlab, GA, USA.

Gel permeation chromatography (GPC). Molecular weight and molecular weight distribution were measured by GPC equipped with a Tosoh EcoSEC HLC 8320GPC system with TSKgel SuperHZ-L columns eluting $CHCl_3$ containing 0.25% triethylamine at a flow rate of 0.45 mL min^{-1}. All number-average molecular weights and dispersities were calculated from refractive index chromatograms using PStQuick Mp-M polystyrene standards.

UV−Vis Absorption Spectroscopy. Absorbance spectra were measured with a Carry 5000 UV−vis/NIR spectrometer. For liquid measurement, the samples were dissolved in anhydrous dichloromethane. For solid-state measurement, the samples were prepared by spincoating the HTM on glass substrates.

Solution Fluorescence Spectroscopy. Fluorescence spectra were measured with a Horiba Jobin Yvon Fluorolog 3-2i spectrometer by dissolving the samples in anhydrous dichloromethane.

Cyclic Voltammetry (CV). Cyclic voltammetry experiments were performed using a BAS potentiostat with a glassy carbon working electrode, platinum counter electrode and an Ag wire reference electrode at a scan rate of 100 mV s^{-1}. Anhydrous and degassed dichloromethane solutions containing 0.1 M of tetrabutylammonium hexafluorophosphate as electrolyte was used to dissolve **M1** (10^{-3} M). Decamethylferrocene was used as the reference.

Differential scanning microscopy (DSC). DSC spectra were measured using a TA Instruments Q200 Differential Scanning Calorimeter and run in the range of 25-200 °C, in nitrogen flow at 5 °C min^{-1} heating rate.

Thermogravimetric analysis (TGA). TGA spectra were measured using a Perkin Elmer Pyris 1 Thermogravimetric Analyzer at 10 °C min^{-1} heating rate and at 20 mL min^{-1} air flow rate.

Scanning electron microscope. SEM images were measured using a FEI Sirion scanning electron microscope at an acceleration voltage of 5 kV.

Current−Voltage Measurements. The *J–V* curves were measured (2400 Series SourceMeter, Keithley Instruments) under simulated AM 1.5 G sunlight at 100 mW cm^{-2}

irradiance generated by an Abet Class AAB sun 2000 simulator, with the intensity calibrated with an NREL calibrated KG 5 filtered Si reference cell. The forward *J–V* scans were measured from forward bias to short circuit and the backward scans were from short circuit to forward bias, both at a scan rate of 380 mV s^{-1}. A stabilization time of 5 s at forward bias of 0 V under illumination was done prior to scanning.

Powder X-ray Diffraction
XRD spectra were measured using a Panalytical X'pert powder diffractometer with Cu anode X-ray source.

Profilometry
The film thickness was measured by stylus profilometry (Bruker Dektak XT).

PL data treatment. Each normalized PL decay was fitted to a stretched exponential function following the method of Stranks *et al*.:[4]

$$I(t) = exp\left[-\left(\frac{t - t_0}{\tau}\right)^{\beta}\right]$$

with I(t) the PL intensity at time t, t_0 an offset correction (constrained such that $0 \leq t0 \leq 10$), τ the characteristic lifetime and β the stretching exponent. The use of a stretched exponential function to fit PL data from perovskite films is well established in the literature, in lieu of a true analytical model.[5, 6] The stretching of the exponential has been interpreted as resulting from a distribution of monomolecular (trap-assisted) non-radiative decay rates within the material.[7] The mean relaxation time, <τ>, given by Equation 4:

$$\langle\tau\rangle = \frac{\tau}{\beta}\Gamma\left(\frac{1}{\beta}\right)$$

where Γ(z) is the gamma function:

$$\Gamma(z) = \int_0^{\infty} x^{z-1}e^{-x}dx$$

Device fabrication
Substrate Preparation. Fluorine-doped tin oxide (FTO) (Pilkington TEC 7) or indium tin oxides (ITO) (Shenzhen Display, < 10 ohm cm^{-2}) coated glass substrates were used in this experiment. FTO or ITO substrates were etched at specific regions using a 2 M HCl and zinc powder. Substrates were then cleaned with water, then sequentially sonicated for 5 min in acetone, isopropyl alcohol and water, and dried with a compressed nitrogen gun. Next, the substrates were treated for 5 min in oxygen plasma.

Electrode Evaporation. An 100 nm silver electrode was thermally evaporated under vacuum.

SnO_2 nanocrystal. We selected a planar SnO_2 nanocrystal deposition procedure that gives us lower power conversion efficiency than SnO_2 chemical bath, but allows the fabrication of devices in a shorter time without requiring high heat or high energy. SnO_2 colloidal precursor (15% in H_2O dispersion) was purchased from Alfa Aesar and diluted in deionized water to 2.7% concentration before use. The dispersion was spin coated onto plasma cleaned FTO substrates at 4000 rpm for 30 s, and then annealed in ambient conditions at 150 °C for 30 min. The SnO_2 films were treated with UV ozone for 10 min immediately prior to perovskite deposition

$Cs_{0.05}FA_{0.95}Pb(I_{0.83}Br_{0.17})_3$ Perovskite. The precursor solution was prepared by dissolving the precursors in anhydrous *N,N*-dimethylformamide and dimethylsulfoxide in a ratio 4:1 in a nitrogen-filled glovebox to obtain a stoichiometric 1.5 M solution. 150 µL of the precursor perovskite solution was spin-coated in a drybox at 1000 rpm for 10 s and then 6000 rpm for 35 s with a ramp of 2000 rpm s^{-1}. After 35 s, 400 µL of toluene was quickly added on the spinning substrates. The films were dried on a hot plate at a temperature of 100 °C for 10 min.

PEA-I passivation layer. To improve the performance of solar cells, the devices with both **P1** and spiro-OMeTAD were further passivated with PEAI by spin coating a solution of 1 mg mL^{-1} in isopropanol at 1000 rpm for 10 s prior to HTM deposition. No additional annealing was performed after depositing PEAI.

Mo(tfd-$COCF_3$)$_3$-Doped P1. A 46 mg mL^{-1} solution of **P1** was prepared in dichlorobenzene in a nitrogen-filled glovebox. The solution was stirred 2 h at 70 °C. Mo(tfd-$COCF_3$)$_3$ in dichlorobenzene (15 mg mL^{-1}) was added accordingly to the molar ratio needed to the polymer solution. Dichlorobenzene was added to adjust the concentration needed. The solution was spin-coated on the perovskite layer at 2500 rpm, 2500 rpm s^{-1} for 45 s in a nitrogen-filled glovebox. The films were dried for 5 minutes at 70 °C.

Li-TFSI Doped P1 or Spiro-OMeTAD. A 85 mg mL^{-1} solution of HTM was prepared in dichlorobenzene in a nitrogen-filled glovebox. The solution was stirred 2h at 70 °C. Li-TFSI in acetonitrile (500 mg mL^{-1}) and 4-*tert*-butylpyridine were added accordingly to the molar ratio needed to the HTM solution. Dichlorobenzene was added to adjust the concentration needed. The solution was spin-coated on the perovskite layer at 2500 rpm, 2500 rpm s^{-1} for 45 s in a nitrogen-filled glovebox. In the case of P1, the best devices were obtained after diluting the solution to 55 mg mL^{-1}, which resulted in film thicknesses of ca. 100 nm, whereas for spiro-OMeTAD, the undiluted solution gave better performing devices and thicknesses of ca. 200 nm.

3. Additional Device Characterization

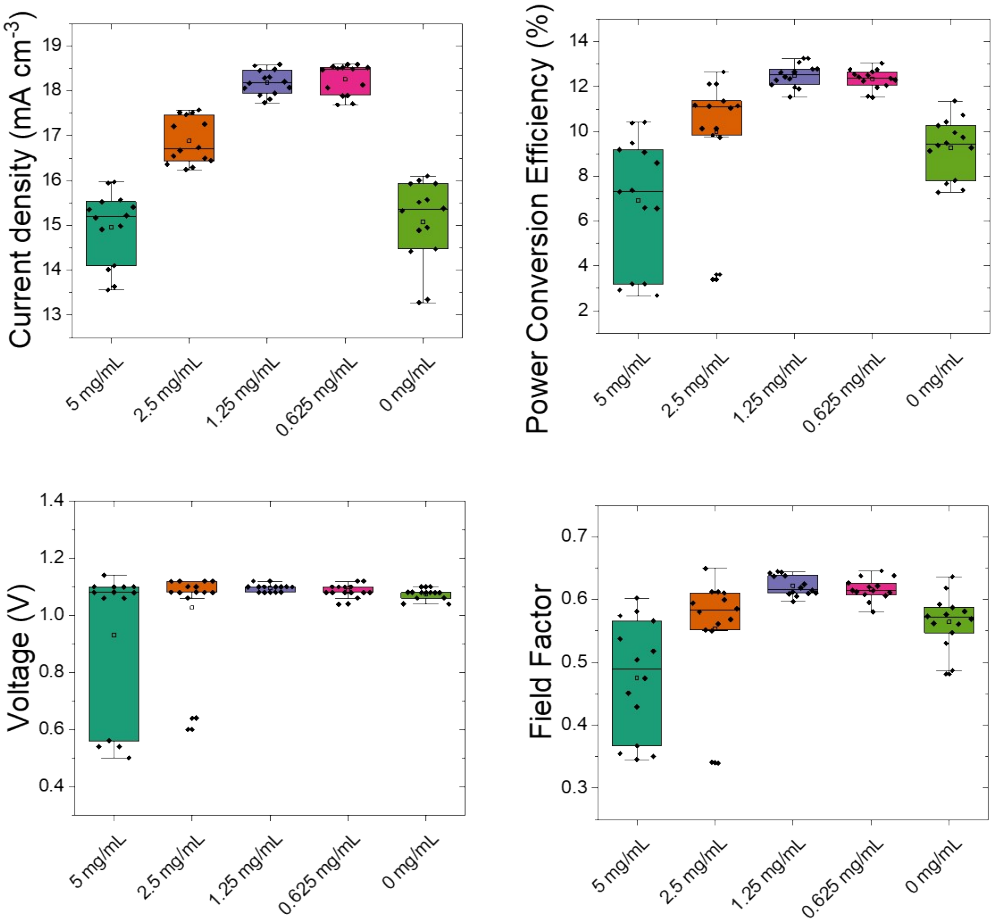

Fig. S1 Comparing the photovoltaic performance of $Cs_{0.05}FA_{0.95}Pb(I_{0.83}Br_{0.17})_3$ devices with different amount of PEA-I passivator. Box-plot of devices prepared in 1 batch showing the comparison of the PV parameters (from J-V curves) of devices at different PEA-I concentration.

Table S1 Statistics for individual $Cs_{0.05}FA_{0.95}Pb(I_{0.83}Br_{0.17})_3$ devices made to optimize PEA-I concentration when **P1** is used as HTM (HTM concentration = 55 mg mL^{-1}).

Concentration PEA-I		J_{sc} (mA cm^{-2})	V_{OC} (V)	FF	PCE (%)
-	Average	15.1 ± 0.9	1.07 ± 0.02	0.56 ± 0.04	9 ± 1
	Maximum	16.1	1.1	0.64	11.4
1.25 mg/mL	Average	18.2 ± 0.3	1.10 ± 0.01	0.62 ± 0.01	12.5 ± 0.5
	Maximum	18.6	1.12	0.65	13.3

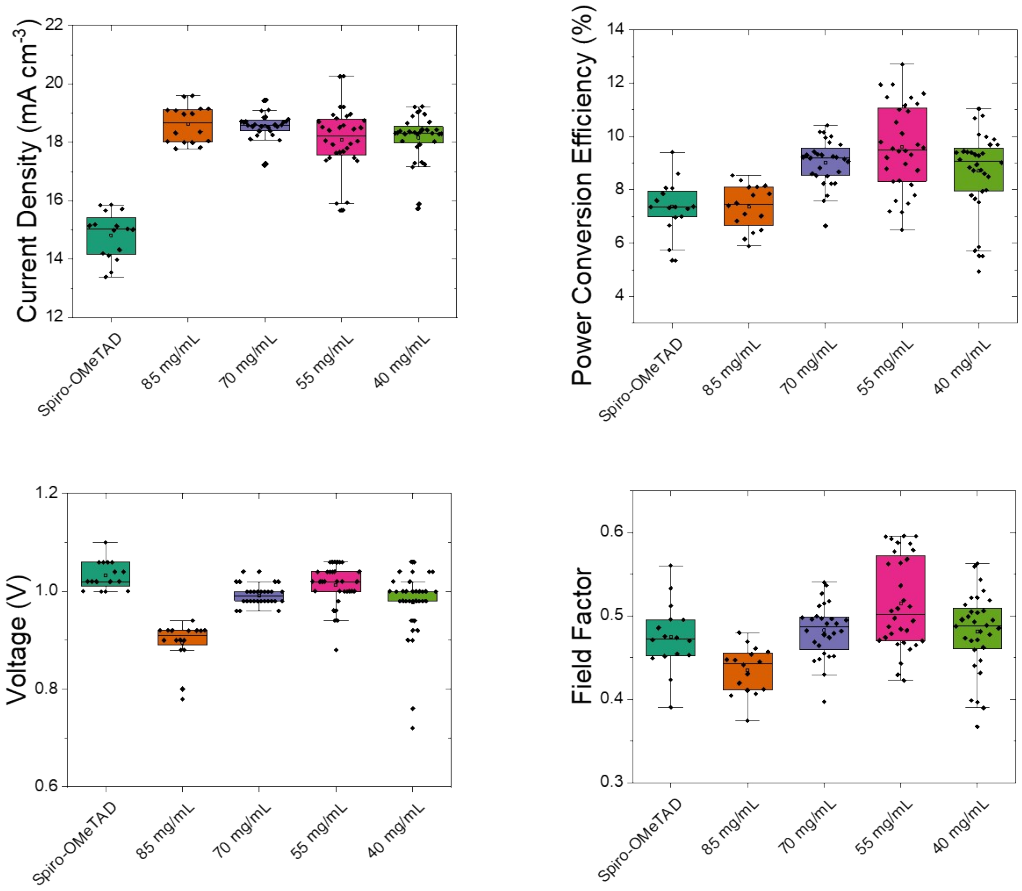

Fig. S2 Comparing the photovoltaic performance of $Cs_{0.05}FA_{0.95}Pb(I_{0.83}Br_{0.17})_3$ devices with different **P1** concentration used to cast 33 mol% Li-doped, 220 mol% *t*BP **P1** films. Box-plot of 16 individual devices for Spiro-OMeTAD and 32 devices for **P1** prepared in 1 batches showing the comparison of the PV parameters (from J-V curves) of devices comprising either Spiro-OMeTAD or **P1** at different concentration as HTM.

Table S2 Statistics for individual $Cs_{0.05}FA_{0.95}Pb(I_{0.83}Br_{0.17})_3$ devices made to optimize **P1** concentration used to cast 33 mol% Li-doped, 220 mol% *t*BP **P1** films.

HTM		J_{sc} (mA cm^{-2})	V_{OC} (V)	FF	PCE (%)
Spiro-OMeTAD reference	Average	14.8 ± 0.8	1.03 ± 0.03	0.47 ± 0.04	7.4 ± 1.0
	Maximum	15.9	1.1	0.56	9.40
P1 55 mg/mL	Average	18 ± 1	1.01 ± 0.04	0.51 ± 0.05	10 ± 2
	Maximum	20.3	1.06	0.60	12.71

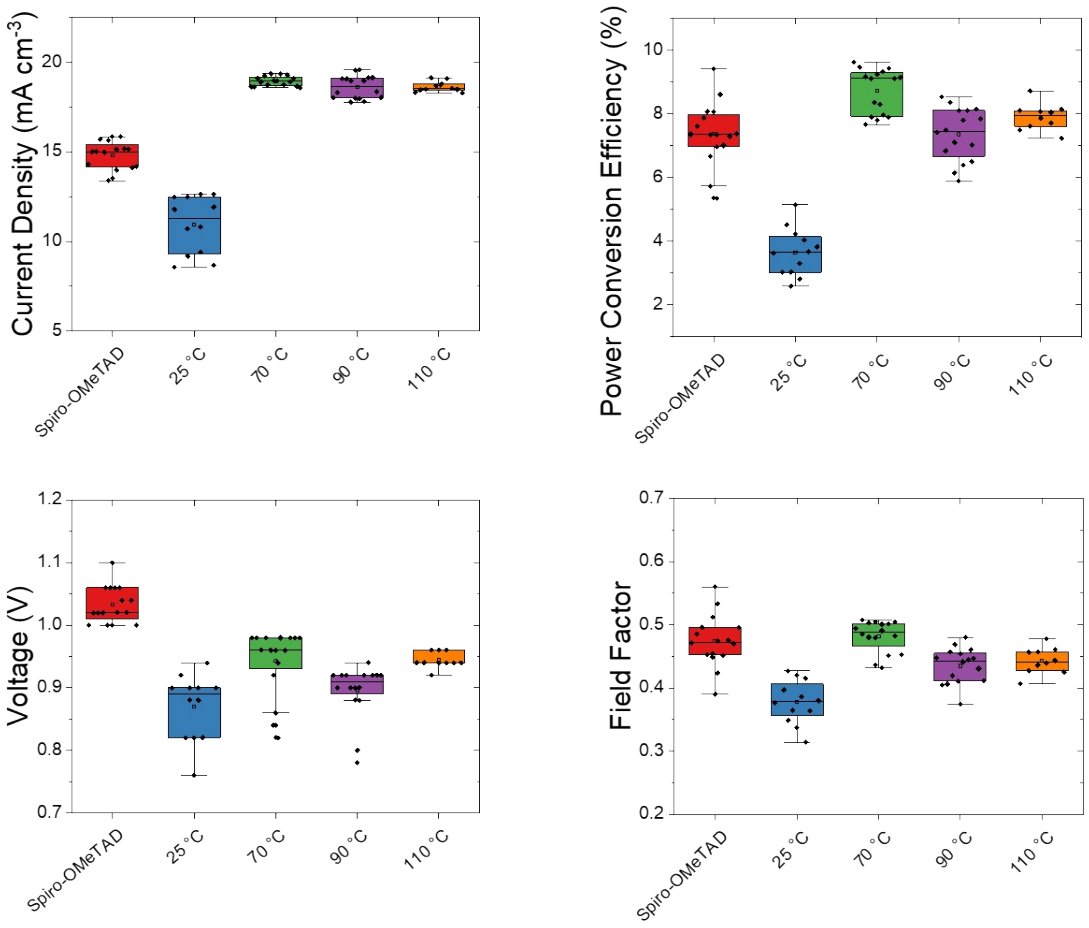

Fig. S3 Comparing the photovoltaic performance of $Cs_{0.05}FA_{0.95}Pb(I_{0.83}Br_{0.17})_3$ devices with different **P1** solution's temperature used to cast 85 mg/mL, 33 mol% Li-doped, 220 mol% *t*BP **P1** films. Box-plot of 16 individual devices prepared in 1 batches showing the comparison of the PV parameters (from J-V curves) of devices comprising either Spiro-OMeTAD or **P1** spun at different temperature as HTM.

Table S3 Statistics for individual $Cs_{0.05}FA_{0.95}Pb(I_{0.83}Br_{0.17})_3$ devices made to optimize **P1** temperature deposition used to cast 85 mg/mL, 33 mol% Li-doped, 220 mol% *t*BP **P1** films.

HTM		J_{sc} (mA cm^{-2})	V_{OC} (V)	FF	PCE (%)
Spiro-OMeTAD reference	Average	14.8 ± 0.8	1.03 ± 0.03	0.47 ± 0.04	7.4 ± 1.0
	Maximum	15.9	1.1	0.56	9.41
P1 70 °C	Average	19.0 ± 0.3	0.94 ± 0.05	0.48 ± 0.03	8.7 ± 0.7
	Maximum	19.4	1.0	0.51	9.63

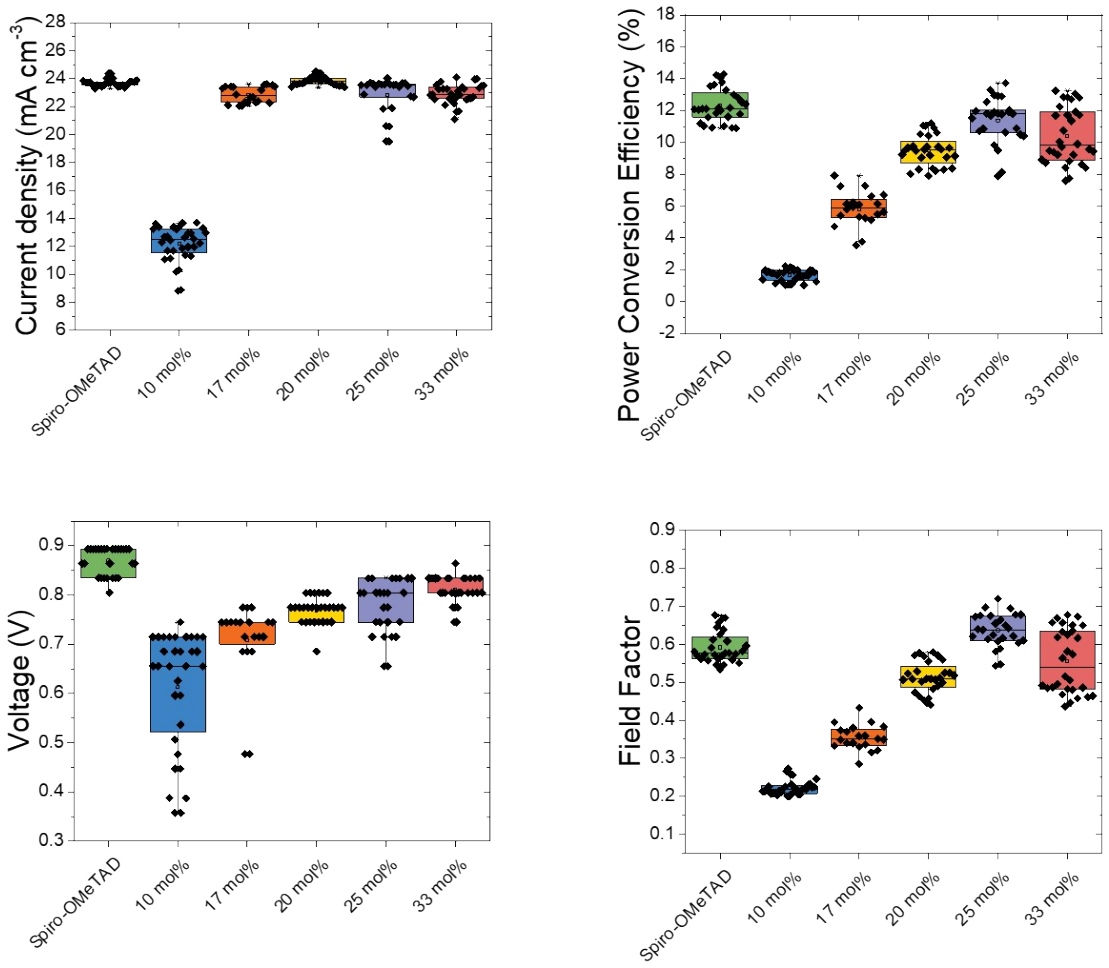

Fig. S4 Comparing the photovoltaic performance of $Cs_{0.05}FA_{0.95}Pb(I_{0.83}Br_{0.17})_3$ devices with different Li-TFSI concentration used to cast 85 mg/mL, 220 mol% *t*BP **P1** films. Box-plot of 26 individual devices prepared in 1 batches showing the comparison of the PV parameters (from J-V curves) of devices comprising either Spiro-OMeTAD or **P1** at different dopant concentration.

Table S4 Statistics for individual $Cs_{0.05}FA_{0.95}Pb(I_{0.83}Br_{0.17})_3$ devices made to optimize **P1** Li-TFSI p-dopant concentration when **P1** is used as HTM (HTM concentration = 85 mg/mL, *t*BP concentration = 220 mol%).

HTM		J_{sc} (mA cm^{-2})	V_{OC} (V)	FF	PCE (%)
Spiro-OMeTAD reference	Average	23.7 ± 0.3	0.87 ± 0.03	0.59 ± 0.04	12 ± 1
	Maximum	24.4	0.90	0.68	14.3
P1 25 mol% Li-TFSI	Average	23 ± 1	0.78 ± 0.06	0.64 ± 0.04	11 ± 1
	Maximum	24.0	0.83	0.72	13.7

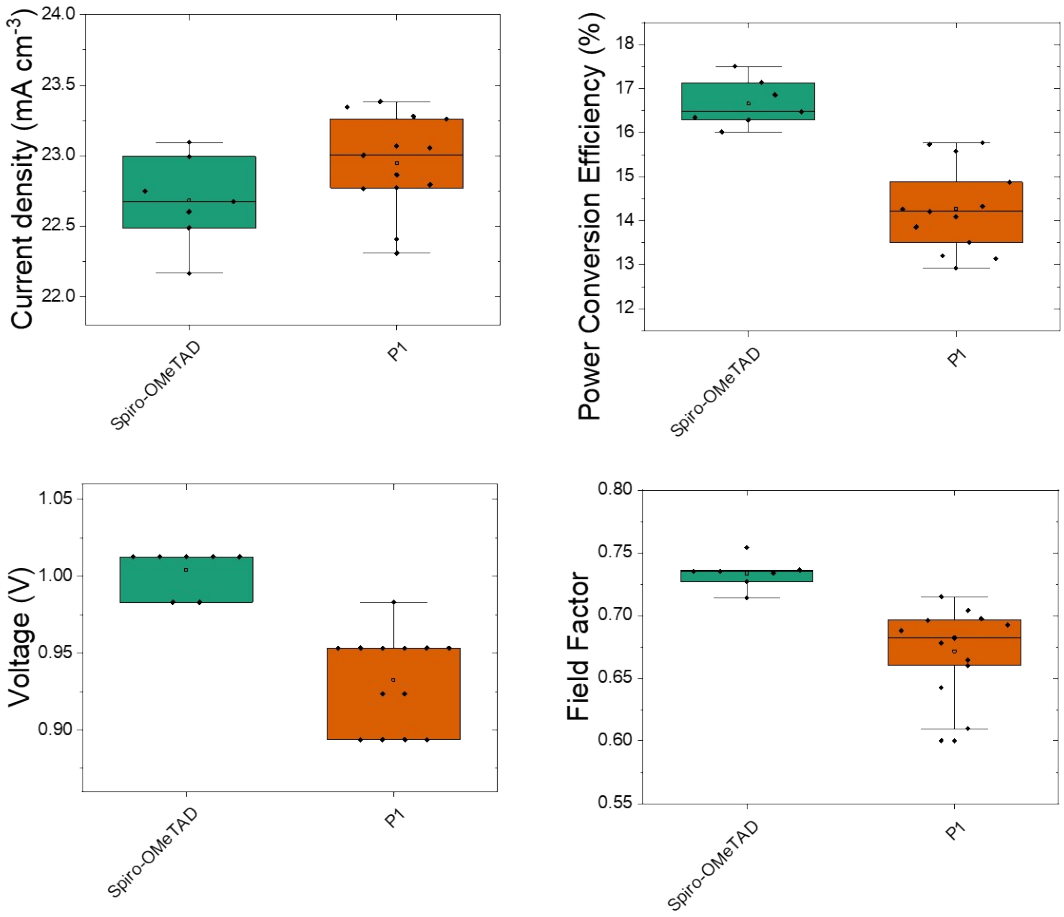

Fig. S5 Comparing the photovoltaic performance of $Cs_{0.05}FA_{0.95}Pb(I_{0.83}Br_{0.17})_3$ devices with Mo(tfd-$COCF_3)_3$ dopant. Box-plot of 13 individual devices prepared in 1 batches showing the comparison of the PV parameters (from J-V curves) of devices comprising either Mo-doped Spiro-OMeTAD or **P1**. Note that the **P1** devices were not fully optimized and this experiment is to present that **P1** devices could be made using another dopant.

Table S5 Statistics for individual $Cs_{0.05}FA_{0.95}Pb(I_{0.83}Br_{0.17})_3$ devices made with Mo(tfd-$COCF_3)_3$ p-dopant when **P1** and Spiro-OMeTAD are used as HTM (HTM concentration = 85 mg/mL).

HTM		J_{sc} (mA cm^{-2})	V_{OC} (V)	FF	PCE (%)
Spiro-OMeTAD Mo-doped	Average	22.7 ± 0.3	1.00 ± 0.01	0.73 ± 0.01	16.7 ± 0.5
	Maximum	23.1	1.01	0.75	17.5
P1 Mo-doped	Average	23.0 ± 0.3	0.93 ± 0.03	0.67 ± 0.04	14.3 ± 0.9
	Maximum	23.4	0.98	0.72	15.8

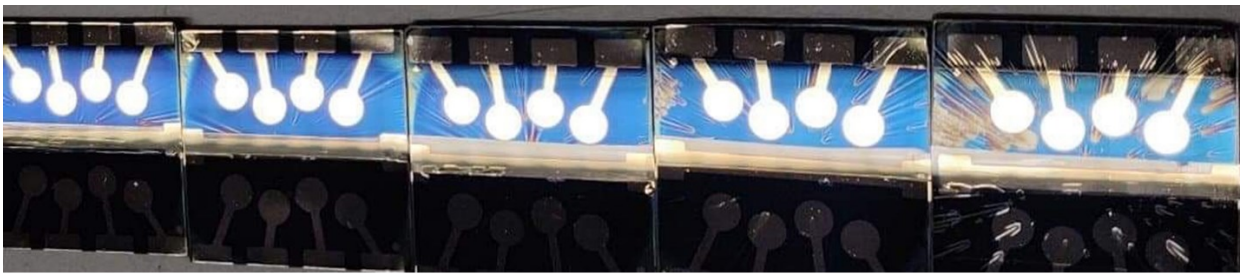

Fig. S6 Optimization of the *t*BP concentration. The lower concentration solution led to a lower density of pinholes, but poorer photovoltaic performance.

References

1. S. A. Paniagua, J. Baltazar, H. Sojoudi, S. K. Mohapatra, S. Zhang, C. L. Henderson, S. Graham, S. Barlow and S. R. Marder, *Materials Horizons*, 2014, **1**, 111-115.
2. S. Samanta, K. Fries, S. Orski and J. Locklin, in *Smart Coatings III*, American Chemical Society, 2010, vol. 1050, ch. 6, pp. 73-85.
3. J.-Y. Cho, B. Domercq, S. Barlow, K. Y. Suponitsky, J. Li, T. V. Timofeeva, S. C. Jones, L. E. Hayden, A. Kimyonok, C. R. South, M. Weck, B. Kippelen and S. R. Marder, *Organometallics*, 2007, **26**, 4816-4829.
4. S. D. Stranks, G. E. Eperon, G. Grancini, C. Menelaou, M. J. P. Alcocer, T. Leijtens, L. M. Herz, A. Petrozza and H. J. Snaith, *Science*, 2013, **342**, 341.
5. G. E. Eperon, S. D. Stranks, C. Menelaou, M. B. Johnston, L. M. Herz and H. J. Snaith, *Energ. Environ. Sci.*, 2014, **7**, 982-988.
6. D. W. de Quilettes, S. M. Vorpahl, S. D. Stranks, H. Nagaoka, G. E. Eperon, M. E. Ziffer, H. J. Snaith and D. S. Ginger, *Science*, 2015, **348**, 683.
7. D. W. deQuilettes, S. Koch, S. Burke, R. K. Paranji, A. J. Shropshire, M. E. Ziffer and D. S. Ginger, *ACS Energy Lett.*, 2016, **1**, 438-444.